



Cite this: *J. Anal. At. Spectrom.*, 2015, **30**, 1400

Received 13th November 2014  
Accepted 11th February 2015

DOI: 10.1039/c4ja00422a

www.rsc.org/jaas

# Minimising $^{12}\text{C}^{3+}$ interference on $^4\text{He}^+$ measurements in a noble gas mass spectrometer

James Schwanethal\*

Measurements of helium isotopes used for geochronological studies are subject to interferences from  $^{12}\text{C}^{3+}$  and  $\text{HD}^+$ . The  $^{12}\text{C}^{3+}$  interference was studied on a Nu Instruments Noblesse mass spectrometer which has sufficient mass resolution to measure the interference on the  $^4\text{He}^+$  peak due to  $^{12}\text{C}^{3+}$  directly, by setting the magnet at the relevant peak shoulders. Helium sensitivity varies with source trap current. Increasing the source trap current increases the electron fluence, and hence the probability of ionisation, within the source. The source trap current on the Noblesse is typically held at  $\sim 400\ \mu\text{A}$ . Increasing the trap current to  $550\ \mu\text{A}$  increases sensitivity to  $^4\text{He}^+$  approximately two-fold, but  $^{12}\text{C}^{3+}$  increases approximately 17 times. The  $^4\text{He}^+$  and  $^{12}\text{C}^{3+}$  peak shoulders at  $m/z = 4$  are narrow, despite the high mass resolution, and consequently any instrument drift can cause the peak positions to be lost. However, it is shown that measurement of  $^{12}\text{C}^{2+}$  at  $m/z = 6$  can be used to correct for this interference, allowing the intensity of the broad flat top of  $m/z = 4$  to be used.

## 1 Introduction

Helium has two naturally occurring isotopes:  $^3\text{He}$  and  $^4\text{He}$ . The ratio of these two isotopes provides valuable insights into various aspects of geochemistry and geochronology.<sup>1–3</sup> Ongoing developments in noble gas research, notably the growing popularity of laser microprobe analysis, prompt noble gas researchers to measure  $^3\text{He}/^4\text{He}$  on ever smaller signals.

The precision of  $^3\text{He}/^4\text{He}$  is generally limited by the  $^3\text{He}^+$  signal, which is nearly always orders of magnitude smaller than  $^4\text{He}^+$ . Increasing sensitivity to  $^3\text{He}^+$  does not only increase the sensitivity to  $^4\text{He}^+$ , but also has the potential to magnify any interference due to  $^{12}\text{C}^{3+}$ . It is therefore desirable to increase the sensitivity to the helium isotopes with minimal, or predictable, effects on the interferences.

One method used to increase the sensitivity to helium is to increase the source trap current,<sup>4</sup> in effect producing more electrons at the filament, and hence more ions within the source, whilst having no effect on electron energy. In doing this it was discovered that as the source trap current increases  $^{12}\text{C}^{3+}$  constitutes an increasingly significant interference at  $m/z = 4$ .

Although the Noblesse mass spectrometer is able to resolve the double peak at  $m/z = 4$ , the peak shoulders on which  $^4\text{He}^+$  (high mass side) and  $^{12}\text{C}^{3+}$  (low mass side) are measured are narrow enough that any short term instrument drift could cause large  $^4\text{He}^+$  measurement errors (Fig. 1). It is therefore desirable

to measure the peak centre, *i.e.*  $^4\text{He}^+ + ^{12}\text{C}^{3+}$ , and find a suitable proxy to enable correction for the  $^{12}\text{C}^{3+}$ . Fortunately  $^{12}\text{C}^{2+}$  provides this proxy.

In this study the effects of changing source trap current on the  $^{12}\text{C}^{3+}$  interference, and the  $^{12}\text{C}^{3+}/^{12}\text{C}^{2+}$  ratio, are investigated. It has previously been shown<sup>5</sup> that as filament voltage, and hence electron energy, increases helium sensitivity shows two maxima in signal intensity, with the highest sensitivity at 90 V. With the resolution of the Noblesse, it is possible to examine the  $m/z = 4$  peak in detail to see the contribution of  $^4\text{He}^+$  and  $^{12}\text{C}^{3+}$  over a range of filament voltages, at various trap currents.

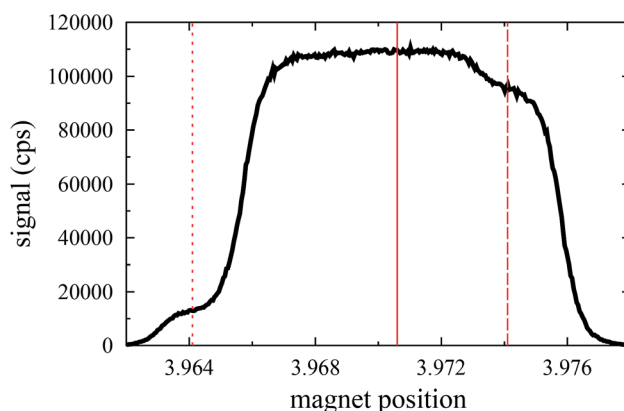


Fig. 1 Resolution of the double peak at  $m/z = 4$  at a trap current of  $550\ \mu\text{A}$ ;  $^{12}\text{C}^{3+}$  is on the lower mass side and  $^4\text{He}^+$  is on the higher mass side. The vertical lines show typical measurement positions on the shoulders of the main peak.

London Geochronology Centre, Department of Earth Sciences, University College London, Gower Street, London, WC1E 6BT, UK. E-mail: J.Schwanethal@ucl.ac.uk



## 2 Method

All measurements were performed on a Nu Instruments Noblesse noble gas mass spectrometer at the London Geochronology Centre (LGC). The Noblesse uses a Nier-type ion source. It employs multi-collection; the LGC Noblesse comprises one Faraday collector (FAR) for large signals and two ion counters (IC0, IC1) for smaller signals. Whilst the location of these detectors is ideally suited to the simultaneous detection of  $^{40}\text{Ar}^+$  (FAR),  $^{38}\text{Ar}^+$  (IC0) and  $^{36}\text{Ar}^+$  (IC1), measurement of the two helium isotopes can also be done in multicollection mode, where  $^4\text{He}^+$  can be detected on FAR and/or IC0 and  $^3\text{He}^+$  on IC0. The software shipped with the mass spectrometer allows the user to produce automated sequence files to control the pneumatic valve system, timings and data analysis. The instrument has a mass resolving power of  $>1000$ , which allows both the  $^3\text{He}^+$  and  $^4\text{He}^+$  interferences,  $\text{HD}^+$  and  $^{12}\text{C}^{3+}$  respectively, to be partially resolved.

A block diagram of the extraction line is shown in Fig. 2. A clean up volume ( $V_C$ ), comprising two SAES getters, one at room temperature ( $G_C$ ) and one at  $400^\circ\text{C}$  ( $G_H$ ) is connected to the mass spectrometer. A laser port with a 213 nm ultraviolet laser grade sapphire viewport (volume  $V_{\text{He}}$ ) is connected to  $V_C$ . The viewport can be isolated from  $V_C$ , and  $V_C$  can be isolated from the mass spectrometer. Typical samples used during *in situ*  $^4\text{He}/^3\text{He}$  analysis were loaded into the sample port to provide realistic blanks and helium signals expected during analysis. There is a liquid nitrogen cold trap between the laser port and the clean up line, which was not used during this experiment in order not to change the sensitivity of the isotopes being measured as the liquid nitrogen in the dewar evaporates.<sup>6</sup> In order to avoid any need for cross calibration between detectors all measurements were made on IC0.

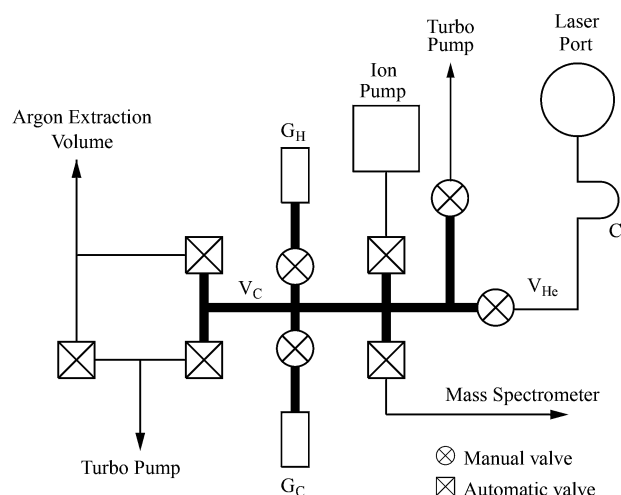


Fig. 2 Helium extraction line at the LGC. The main volume  $V_C$  (bold line) has one getter at  $400^\circ\text{C}$  ( $G_H$ ) and one getter at room temperature ( $G_C$ ). On the right hand side of the main volume is the 'helium' extraction line,  $V_{\text{He}}$ , where a sapphire, or fused silica, ultraviolet grade windowed laser port is connected *via* a liquid nitrogen cold trap, C. Samples are ablated by a New Wave 213 nm laser.

### 2.1 Varying trap current

The mass spectrometer was tuned at trap currents from  $250\ \mu\text{A}$  to  $550\ \mu\text{A}$  in  $50\ \mu\text{A}$  increments. The source and filament voltages were kept constant at  $5994\ \text{V}$  and  $-94\ \text{V}$  respectively. Half plate and repeller voltages were tuned to give maximum signal – half plate voltage was 82.5% of source voltage at  $250\ \mu\text{A}$ , 88.1% at  $450\ \mu\text{A}$  and 87.3% at  $550\ \mu\text{A}$ . The tuning settings at each value of trap current were saved to file, allowing rapid adjustment between analyses. A heating effect was observed when raising the trap current (and consequently the filament current). The trap current was therefore dropped from  $550\ \mu\text{A}$  to  $250\ \mu\text{A}$  over the course of the day. The peak positions were checked, and if necessary corrected, several times a day and each day before starting measurements to check for any drift in the mass spectrometer. The trap current was returned to  $550\ \mu\text{A}$  at the end of each day, allowing the source to stabilise overnight. It was observed that carbon background was highest after turning up the trap current, and reduced over subsequent days. This is presumably due to the filament heating the volume surrounding it, outgassing any surface carbon or hydrocarbons.

Three sets of runs were carried out, using the sequence files described in Sections 2.1.1 and 2.1.2: Run 1 measured  $^4\text{He}^+$  and  $^{12}\text{C}^{3+}$  at blank level, Run 2 measured  $^{12}\text{C}^{2+}$  and  $^{12}\text{C}^{3+}$  at blank level, and Run 3 measured  $^4\text{He}^+$  and  $^{12}\text{C}^{3+}$  at typical sample level.

**2.1.1  $^4\text{He}^+$  and  $^{12}\text{C}^{3+}$  measurement.** For Run 1 the laser port and  $V_C$  were isolated from the ion pump. No additional sample gas was added to the line.  $V_C$  was left to clean up for two minutes, and the inlet valve was then opened admitting gas into the mass spectrometer; 'time zero' was set at this point. After 30 s of equilibration  $V_C$  was isolated from the mass spectrometer. The analysis file was then run. This analysis file measured the signal at four magnet settings by peak hopping: Baseline,  $^4\text{He}^+$ ,  $^4\text{He}^+ + ^{12}\text{C}^{3+}$  and  $^{12}\text{C}^{3+}$ . Ten cycles of ten measurements were made at each magnet setting. Signals were then regressed to time zero, in common with normal practice for noble gas geochemistry. At the end of the measurement, the mass spectrometer and  $V_C$  were opened to the ion pumps. The trap current was lowered by  $50\ \mu\text{A}$ , and the above sequence re-run. This procedure carried on until a trap current of  $250\ \mu\text{A}$  was reached.

For Run 3 a GJ1 zircon<sup>7</sup> was laser ablated to release  $\sim 65\ 000$  cps of  $^4\text{He}^+$  into  $V_C$ . This sample gas was cleaned up over two minutes in  $V_C$  and then admitted to the mass spectrometer over 30 s. Once the inlet valve was shut the measurement sequence above was run, but the gas in the mass spectrometer was retained, the trap current dropped by  $50\ \mu\text{A}$  and the analysis file rerun. In this way, the analysis was carried out over the same sample gas, the rate of consumption of  $^4\text{He}^+$  in the mass spectrometer being low over the 45 minute duration of the experiment.

**2.1.2  $^{12}\text{C}^{3+}$  and  $^{12}\text{C}^{2+}$  sequence.** An initial check was made to see the contributions of the mass spectrometer volume, the clean up volume ( $V_C$ ) and the helium line volume ( $V_{\text{He}}$ ) to the background  $^{12}\text{C}^{2+}$  level. To reduce the  $^{12}\text{C}^{2+}$  signal at high trap currents,  $V_{\text{He}}$  was isolated from  $V_C$ . The same analysis protocol was followed as for Run 1 above, the only difference being that



the analysis file measured the signal at three magnet positions: baseline,  $^{12}\text{C}^{3+}$  and  $^{12}\text{C}^{2+}$ . In addition, the measurement sequence was run at 550  $\mu\text{A}$  trap current and  $-94\text{ V}$  filament voltage over a range of  $^{12}\text{C}^{2+}$  signal intensities.

## 2.2 Varying filament voltage for a range of trap currents

At the start of the day, with the source trap current set to 550  $\mu\text{A}$ , and filament voltage to  $-94\text{ V}$ , a sample of GJ1 zircon was laser ablated for 5 seconds to release 80 000 to 100 000 cps of  $^4\text{He}^+$  into the mass spectrometer. The clean up line was then closed to the mass spectrometer, and the source trap current set to 550  $\mu\text{A}$  and filament voltage to  $-100\text{ V}$ . The  $^4\text{He}$  in the mass spectrometer was used to tune the peaks at filament voltages from  $-100\text{ V}$  to  $-45\text{ V}$  in 5 V increments, seeking to maximise the ( $^{12}\text{C}^{3+} + ^4\text{He}^+$ ) signal, rather than achieve the 'best' peak shape; each tuning setup was saved to file. A scan at  $m/z = 4$  was performed at each filament voltage to check the position of the  $^4\text{He}^+$  and  $^{12}\text{C}^{3+}$  shoulders.

A shorter version of the  $^4\text{He}^+$  and  $^{12}\text{C}^{3+}$  sequence was run (Section 2.1.1), which contained five cycles of ten measurements for a total analysis time of 216 s. The sequence file was run at filament voltages from  $-100\text{ V}$  down to  $-45\text{ V}$ , in 5 V increments, using the saved tuning settings. The total time duration between the first and last analysis was less than 30 minutes, the effect of any consumption of  $^4\text{He}^+$  on the overall change in signal being minimised. The trap current was then reset to 550  $\mu\text{A}$ , and filament voltage to  $-94\text{ V}$  and left to stabilise overnight. The above procedure was then repeated over two days for 450  $\mu\text{A}$  and 250  $\mu\text{A}$ .

## 3 Results

### 3.1 Varying trap current

The measurements reveal a change in sensitivity over a range of trap currents which increases from  $^4\text{He}^+$  to  $^{12}\text{C}^{2+}$  and  $^{12}\text{C}^{3+}$

(Fig. 3). The change in sensitivity for  $^4\text{He}^+$  is consistent across a broad range of signals.

Although the  $^{12}\text{C}^{3+}$  signal, and hence  $^4\text{He}^+$  interference, increases with trap current, the  $^{12}\text{C}^{2+} : ^{12}\text{C}^{3+}$  ratio becomes more consistent (Fig. 4). Therefore it is possible to use the  $^{12}\text{C}^{2+}$  as (i) an indication of potential  $^{12}\text{C}^{3+}$  interference on the  $^4\text{He}^+$  peak, and (ii) with sufficient calibration data over a wide range of intensities, the  $^{12}\text{C}^{2+}$  signal can be used to correct for interferences on  $^4\text{He}^+$ . This allows the  $^4\text{He}^+ + ^{12}\text{C}^{3+}$  peak centre to be used for measurements, and avoids the technical difficulties with measuring a narrow peak shoulder.

### 3.2 Varying filament voltage

Fig. 5 shows peak shapes at selected filament voltages at three trap currents: 250  $\mu\text{A}$ , 450  $\mu\text{A}$  and 550  $\mu\text{A}$ . At higher filament voltages a slight gradient on the flat top of the peak can be seen. This is due to the slow magnet sweep across the peak, and the  $^{12}\text{C}^{3+}$  variation over time as it continues to outgas from, as well as be consumed by, the mass spectrometer. At low filament voltages, where there is virtually no contribution from  $^{12}\text{C}^{3+}$ , there is a flat top and the peak is predominantly  $^4\text{He}^+$ .

At a trap current of 250  $\mu\text{A}$ , the electron fluence is sufficiently low that there is effectively no contribution from  $^{12}\text{C}^{3+}$ . This results in single peaks, with a flat top. As the trap current increases, the  $^{12}\text{C}^{3+}$  shoulder can be seen to appear on the low mass side of the peak. At 450  $\mu\text{A}$  the contribution is relatively small, but at 550  $\mu\text{A}$ , the shoulder becomes more pronounced.

Fig. 6 shows the intensities at the centre of the main peak, as well as the  $^{12}\text{C}^{3+}$  and  $^4\text{He}^+$  shoulders for the three trap currents. In all cases the main peak shows two maxima, which are most pronounced in the case of 250  $\mu\text{A}$  where the peak is made up of only  $^4\text{He}^+$ . Table 1 shows the ionisation energy for He and C. The first ionisation energy for He occurs at 24.59 eV, and the

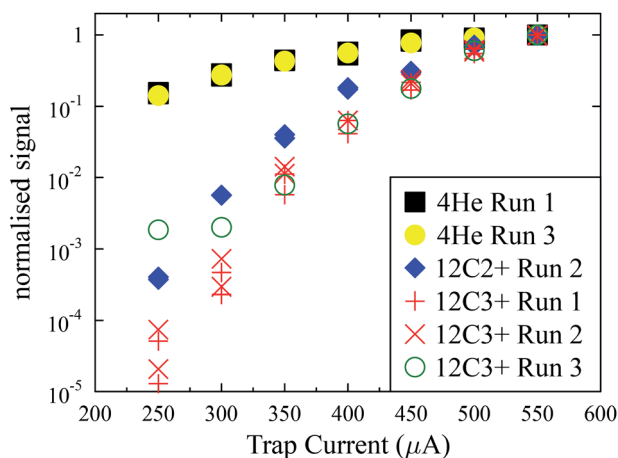


Fig. 3 Normalised signals for  $^4\text{He}^+$ ,  $^{12}\text{C}^{2+}$  and  $^{12}\text{C}^{3+}$  as a function of source trap current. Runs 1 and 2 were at blank level ( $^4\text{He}^+ \approx 100\text{ cps}$  at 550  $\mu\text{A}$ ); Run 3 was of the order of magnitude of a typical sample ( $^4\text{He}^+ \approx 65\,000\text{ cps}$  at 550  $\mu\text{A}$ ). The tail at the low mass end of the  $^4\text{He}^+$  peak limits measurement of  $^{12}\text{C}^{3+}$  at 250 and 300  $\mu\text{A}$ .

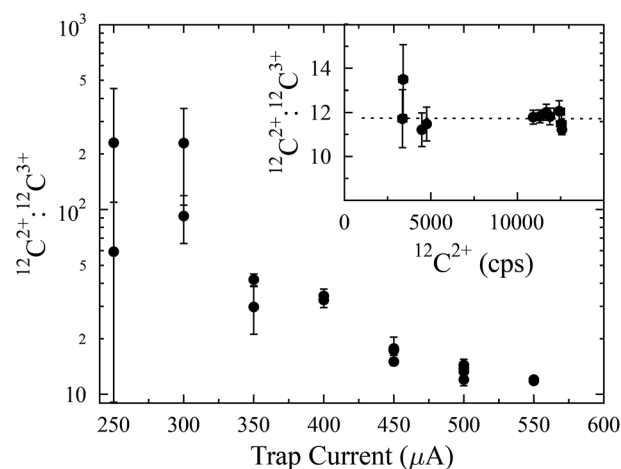


Fig. 4  $^{12}\text{C}^{2+} : ^{12}\text{C}^{3+}$  signal ratio as a function of trap current. Below 300  $\mu\text{A}$  the  $^{12}\text{C}^{3+}$  signal is small, and the uncertainties on the 2+ : 3+ ratios become significant. The inset plot shows the 2+ : 3+ ratio as a function of  $^{12}\text{C}^{2+}$  intensity at a trap current of 550  $\mu\text{A}$ .



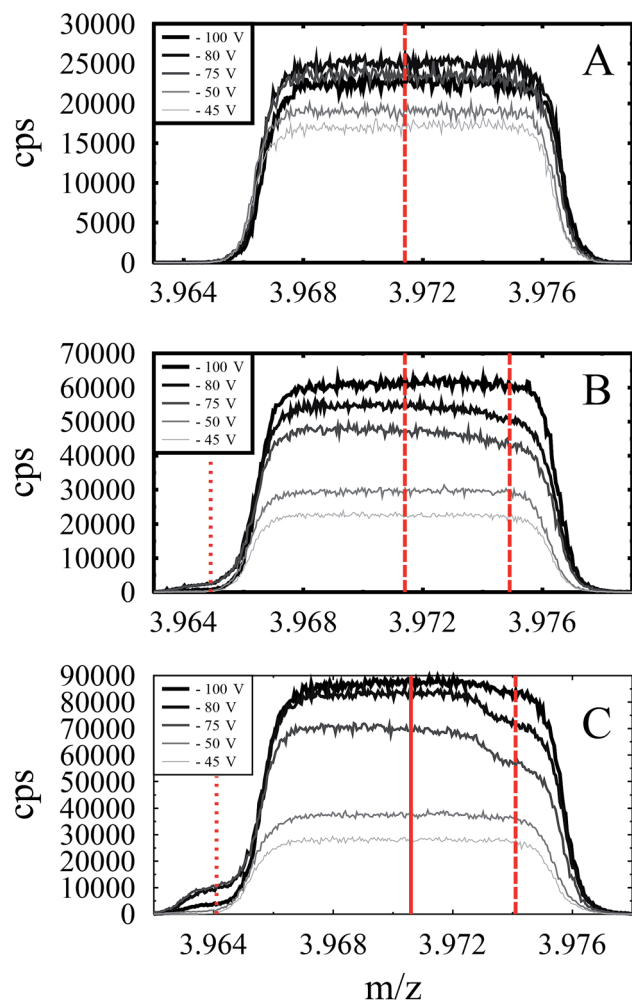


Fig. 5 Peak shape as a function of filament voltage for 250  $\mu\text{A}$  (A), 450  $\mu\text{A}$  (B), and 550  $\mu\text{A}$  (C) trap currents. Vertical lines show the peak positions for  $^{12}\text{C}^{3+}$  (dotted),  $(^{12}\text{C}^{3+} + ^4\text{He}^+)$  (solid) and  $^4\text{He}^+$  (dashed). A perfect 'flat top' peak is only visible when there is no  $^{12}\text{C}^{3+}$  interference, due to the short term variation in the  $^{12}\text{C}^{3+}$  signal.

second at 54.42 eV. The first maximum occurs at 55 V (Fig. 6), the subsequent drop in sensitivity at 60 V could be due to  $^4\text{He}^+$  being doubly ionised. There follows however a secondary maximum at 85 V. It has been suggested<sup>5</sup> that this secondary maximum is due to the electrons having sufficient energy at higher filament voltages to create secondary electrons from electron-metal collisions in the ion source.

As the trap current increases, the two maxima still occur but are less well defined. The second maximum occurs at approximately 90 V. However, as trap current increases, the  $^{12}\text{C}^{3+}$  component becomes more significant, with a maximum intensity at a filament voltage of 75 V. Once this contribution to the signal is taken into account, it can be seen that the  $^4\text{He}^+$  signal intensity continues to rise above 100 V (the maximum working voltage of the mass spectrometer).

The third ionisation energy for C is 47.89 eV (Table 1).  $^{12}\text{C}^{3+}$  increases from 50 V, peaks at 75 V, and then drops off in a similar manner to  $^4\text{He}^+$  at 55 V (Fig. 6C). However in the case of  $^{12}\text{C}^{3+}$ , there is no second maximum below 100 V. The 4th

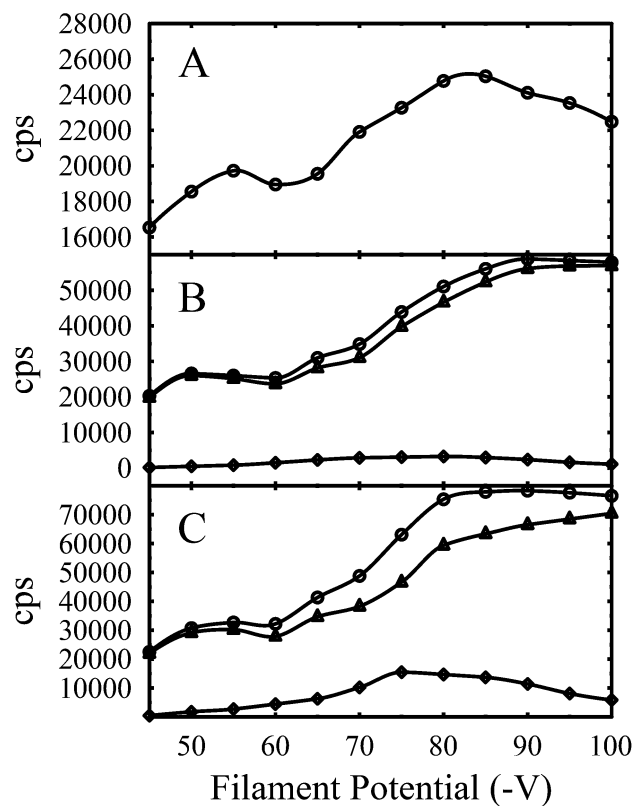


Fig. 6  $^4\text{He}^+$  ( $\Delta$ ),  $(^{12}\text{C}^{3+} + ^4\text{He}^+)$  (O) and  $^{12}\text{C}^{3+}$  ( $\diamond$ ) peak intensities for: (A) 250  $\mu\text{A}$ , (B) 450  $\mu\text{A}$  and (C) 550  $\mu\text{A}$  trap currents. For 250  $\mu\text{A}$ ,  $^{12}\text{C}^{3+}$  is not observed, so the peak centre represents  $^4\text{He}^+$  only.

Table 1 Ionisation energies for helium and carbon<sup>a</sup>

Element	1st	2nd	3rd	4th
He	24.59	54.42	n/a	n/a
C	11.26	24.38	47.89	64.49

ionisation energy for carbon is, at 64.49 eV, within the range of filament voltages used to explain this reduction in intensity above 75 V.

## 4 Conclusions

This paper has documented the effects of an isobaric interference on  $^4\text{He}^+$  by  $^{12}\text{C}^{3+}$ . The magnitude of this interference monotonically rises with increasing trap current, and may significantly bias  $^4\text{He}^+$  measurements if uncorrected for. It has been shown this interference can reliably be removed by monitoring  $^{12}\text{C}^{2+}$  during the measurement. This correction is based on the observation that the  $^{12}\text{C}^{2+} : ^{12}\text{C}^{3+}$  ratio asymptotically approaches a constant value at high trap currents.

There are differences in the increases in yield for  $^4\text{He}^+$ ,  $^{12}\text{C}^{2+}$  and  $^{12}\text{C}^{3+}$  as trap current increases. This can be explained by the number of interactions that must take place to produce these ions.  $^4\text{He}$ , as a noble gas, does not form molecules and requires



only one sufficiently high energy electron to ionise it. C will derive from hydrocarbons and C within the mass spectrometer. Hydrocarbon bonds are broken within the source, then ionised. Therefore multiple electron interactions are required; it follows that given  $^{12}\text{C}^{3+}$  requires one more electron interaction than  $^{12}\text{C}^{2+}$  means the yield will be lower. With a sufficiently high fluence of electrons produced by the filament the efficiency of breaking bonds and multiple ionisation increases.

There needs to be a balance between high trap currents for increased sensitivity and low trap currents for lower interference. In either case, it makes sense to use higher filament voltages, tuned for highest  $^4\text{He}^+$  sensitivity, which at higher trap currents is not necessarily the highest  $m/z = 4$  (i.e.  $^{12}\text{C}^{3+} + ^4\text{He}^+$ ) sensitivity. If it is desirable to have the highest sensitivity to helium by increasing the trap current, then it becomes important to monitor the carbon interference. If the peak shoulders are not wide enough to measure reliably, then a proxy for the  $^{12}\text{C}^{3+}$  must be used. This paper has shown that the  $^{12}\text{C}^{2+}$  at  $m/z = 6$  can be used for this purpose and the ratio of the  $^{12}\text{C}^{2+} : ^{12}\text{C}^{3+}$  signals are constant at higher trap currents.

Changing the trap current will require the source to be retuned; modifications were made to half plate and repeller voltages, at a constant source voltage. Further tuning is then required to optimise the peak shape at the expense of intensity. Increasing trap current increases local heating, and unfortunately reduces the lifetime of the filament. If mass resolution is not available to distinguish between the peaks, then a low trap current may be desirable. Fig. 6A and C show that, if a 'pure'  $^4\text{He}^+$  peak is required, then the a low trap current and high filament voltage (250  $\mu\text{A}$  and 85 V respectively) produces a similar response to high trap current and low filament voltage (550  $\mu\text{A}$  and 45 V or 450  $\mu\text{A}$  and 50 V, respectively). The tuning parameters to be used will ultimately depend on the application, and the interferences may not be applicable to all noble gas mass spectrometers. However, consideration should be

given, when increasing source trap current in order to increase signal intensity, to the potential consequences on the interfering species.

## Acknowledgements

This research was funded by ERC Starting Grant 259504 ('KArSD'). Components for the helium line were funded through NERC grant NE/K003232/1. Pieter Vermeesch and Yuntao Tian provided suitable helium rich samples, and John Saxton at Nu Instruments is thanked for helpful insights into the Noblesse. Two anonymous reviewers are thanked for improving the manuscript.

## References

- 1 M. Ozima and F. A. Podosek, *Noble gas geochemistry*, Cambridge University Press, 2002.
- 2 D. Porcelli, C. J. Ballentine and R. Wieler, *Noble gases in geochemistry and cosmochemistry*, Mineral Soc America, 2002.
- 3 D. L. Shuster and K. A. Farley, *Earth Planet. Sci. Lett.*, 2004, **217**, 1–17.
- 4 W. H. Amidon and K. A. Farley, *Geochem., Geophys., Geosyst.*, 2010, **11**, Q10004.
- 5 J. Mabry, P. Burnard, P.-H. Blard and L. Zimmermann, *J. Anal. At. Spectrom.*, 2012, **27**, 1012–1017.
- 6 J. Mabry, T. Lan, P. Burnard and B. Marty, *J. Anal. At. Spectrom.*, 2013, **28**, 1903–1910.
- 7 S. E. Jackson, N. J. Pearson, W. L. Griffin and E. A. Belousova, *Chem. Geol.*, 2004, **211**, 47–69.
- 8 A. Kramida, Y. Ralchenko and J. Reader, *NIST ASD Team, NIST Atomic Spectra Database (ver. 5.2)*, [Online], Available: <http://physics.nist.gov/asd> [2014, October 10], National Institute of Standards and Technology, Gaithersburg, MD., 2014.

